Systems Dynamic Modeling of a Guard Cell Cl^- Channel Mutant Uncovers an Emergent Homeostatic Network Regulating Stomatal Transpiration[1][W][OA]

Yizhou Wang, Maria Papanatsiou, Cornelia Eisenach, Rucha Karnik, Mary Williams, Adrian Hills, Virgilio L. Lew, and Michael R. Blatt*

Laboratory of Plant Physiology and Biophysics, Institute of Molecular, Cell, and Systems Biology, University of Glasgow, Glasgow G12 8QQ, United Kingdom (Y.W., M.P., C.E., R.K., M.W., A.H., M.R.B.); American Society of Plant Biologists, Rockville, Maryland 20855 (M.W.); and Physiological Laboratory, University of Cambridge, Cambridge CB2 3EG, United Kingdom (V.L.L.)

Stomata account for much of the 70% of global water usage associated with agriculture and have a profound impact on the water and carbon cycles of the world. Stomata have long been modeled mathematically, but until now, no systems analysis of a plant cell has yielded detail sufficient to guide phenotypic and mutational analysis. Here, we demonstrate the predictive power of a systems dynamic model in Arabidopsis (*Arabidopsis thaliana*) to explain the paradoxical suppression of channels that facilitate K^+ uptake, slowing stomatal opening, by mutation of the SLAC1 anion channel, which mediates solute loss for closure. The model showed how anion accumulation in the mutant suppressed the H^+ load on the cytosol and promoted Ca^{2+} influx to elevate cytosolic pH (pH_i) and free cytosolic Ca^{2+} concentration ($[Ca^{2+}]_i$), in turn regulating the K^+ channels. We have confirmed these predictions, measuring pH_i and $[Ca^{2+}]_i$ in vivo, and report that experimental manipulation of pH_i and $[Ca^{2+}]_i$ is sufficient to recover K^+ channel activities and accelerate stomatal opening in the *slac1* mutant. Thus, we uncover a previously unrecognized signaling network that ameliorates the effects of the *slac1* mutant on transpiration by regulating the K^+ channels. Additionally, these findings underscore the importance of H^+-coupled anion transport for pH_i homeostasis.

Guard cells surround stomatal pores in the epidermis of plant leaves and regulate pore aperture to balance the demands for CO_2 in photosynthesis with the need to conserve water by the plant. Transpiration through stomata accounts for much of the 70% of global water usage associated with agriculture, and it has a profound impact on the water and carbon cycles of the world (Gedney et al., 2006; Betts et al., 2007). Guard cells open the pore by transport and accumulation of osmotically active solutes, mainly K^+ and Cl^- and the organic anion $malate^{2-}$ (Mal), to drive water uptake and cell expansion. They close the pore by coordinating the release of these solutes through K^+ and anion channels at the plasma membrane. The past half-century has generated a wealth of knowledge on guard cell transport, signaling, and homeostasis, resolving the properties of the major transport processes and metabolic pathways for osmotic solute uptake and accumulation, and many of the signaling pathways that control them (Blatt, 2000; Schroeder et al., 2001; McAinsh and Pittman, 2009; Hills et al., 2012). Even so, much of stomatal dynamics remains unresolved, especially how the entire network of transporters in guard cells works to modulate solute flux and how this network is integrated with organic acid metabolism (Wang and Blatt, 2011) to achieve a dynamic range of stomatal apertures.

This gap in understanding is most evident in a number of often unexpected observations, many of which have led necessarily to ad hoc interpretations. Among these, recent studies highlighted a diurnal variation in the free cytosolic Ca^{2+} concentration ($[Ca^{2+}]_i$), high in the daytime despite the activation of primary ion-exporting ATPases, and have been interpreted to require complex levels of regulation (Dodd et al., 2007). Other findings wholly defy intuitive explanation. For example, the *tpk1* mutant of Arabidopsis (*Arabidopsis thaliana*) removes a major pathway for K^+ flux across the tonoplast and suppresses stomatal closure, yet the mutant has no significant effect on cellular K^+ content (Gobert et al., 2007). Similarly, the Arabidopsis *clcc* mutant eliminates the H^+-Cl^- antiporter at the tonoplast; it affects Cl^- uptake, reduces vacuolar Cl^- content, and slows stomatal opening; however, counterintuitively, it also suppresses stomatal closure (Jossier et al., 2010). In work leading to this study, we observed that the *slac1* anion channel mutant of Arabidopsis paradoxically profoundly alters the activities

[1] This work was supported by the Biotechnology and Biological Sciences Research Council (grant nos. BB/H024867/1, BB/F001630/1, and BB/H009817/1 to M.R.B.), by a Chinese Scholarship Council and Glasgow University PhD scholarship to Y.W., and by a Begonia Trust PhD studentship to M.P.

* Corresponding author; e-mail michael.blatt@glasgow.ac.uk.

The author responsible for distribution of materials integral to the findings presented in this article in accordance with the policy described in the Instructions for Authors (www.plantphysiol.org) is: Michael R. Blatt (michael.blatt@glasgow.ac.uk).

[W] The online version of this article contains Web-only data.

[OA] Open Access articles can be viewed online without a subscription.

www.plantphysiol.org/cgi/doi/10.1104/pp.112.207704

of the two predominant K^+ channels at the guard cell plasma membrane. The *SLAC1* anion channel is a major pathway for anion loss from the guard cells during stomatal closure (Negi et al., 2008; Vahisalu et al., 2008), and its mutation leads to incomplete and slowed closure of stomata in response to physiologically relevant signals of dark, high CO_2, and the water-stress hormone abscisic acid. Guard cells of the *slac1* mutant accumulate substantially higher levels of Cl^-, Mal, and also K^+ when compared with guard cells of wild-type Arabidopsis (Negi et al., 2008). The latter observation is consistent with additional impacts on K^+ transport; however, a straightforward explanation for these findings has not been not forthcoming.

Quantitative systems analysis offers one approach to such problems. Efforts to model stomatal function generally have been driven by a "top-down" approach (Farquhar and Wong, 1984; Eamus and Shanahan, 2002) and have not incorporated detail essential to understanding the molecular and cellular mechanics that drive stomatal movement. Only recently we elaborated a quantitative systems dynamic approach to modeling the stomatal guard cell that incorporates all of the fundamental properties of the transporters at the plasma membrane and tonoplast, the salient features of osmolite metabolism, and the essential cytosolic pH (pH_i) and $[Ca^{2+}]_i$ buffering characteristics that have been described in the literature (Hills et al., 2012). The model resolved with this approach (Chen et al., 2012b) successfully recapitulated a wide range of known stomatal behaviors, including transport and aperture dependencies on extracellular pH, KCl, and $CaCl_2$ concentrations, diurnal changes in $[Ca^{2+}]_i$ (Dodd et al., 2007), and oscillations in membrane voltage and $[Ca^{2+}]_i$ thought to facilitate stomatal closure (Blatt, 2000; McAinsh and Pittman, 2009; Chen et al., 2012b). We have used this approach to resolve the mechanism behind the counterintuitive alterations in K^+ channel activity uncovered in the *slac1* mutant of Arabidopsis. Here, we show how anion accumulation in the mutant affects the H^+ and Ca^{2+} loads on the cytosol, elevating pH_i and $[Ca^{2+}]_i$, and in turn regulating the K^+ channels. We have validated the key predictions of the model and, in so doing, have uncovered a previously unrecognized homeostatic network that ameliorates the effects of the *slac1* mutant on transpiration from the plant.

RESULTS

A Cl^- Channel Mutation Alters the Activities of K^+ Channels and Slows Stomatal Opening

The uptake and release of K^+ across the guard cell plasma membrane is mediated largely by two subsets of voltage-gated or Kv-like K^+ channels. Channels mediating K^+ uptake are dominated by the *KAT1* K^+ channel gene product in Arabidopsis, and they give rise to an inward-rectifying (inward-directed) K^+ current ($I_{K,in}$) that activates at voltages near and negative of −120 mV. K^+ release in Arabidopsis occurs through the GORK K^+ channel that gives rise to an outward-rectifying (outward-directed) K^+ current ($I_{K,out}$) at voltage positive of the K^+ equilibrium voltage (Blatt, 1988, 2000; Schachtman et al., 1992; Nakamura et al., 1995; Blatt and Gradmann, 1997; Ache et al., 2000; Schroeder et al., 2001; Hosy et al., 2003). On recording $I_{K,in}$ and $I_{K,out}$ under voltage clamp (Chen et al., 2012a), we observed the profound suppression of $I_{K,in}$ and moderate enhancement of $I_{K,out}$ in intact guard cells of *slac1-1* mutant Arabidopsis compared with currents from guard cells of wild-type and *pSLAC1*::*SLAC1*-complemented *slac1-1* mutant (hereafter referred to as *pSLAC1*) plants (Vahisalu et al., 2008). Guard cells of wild-type and *pSLAC1* plants showed similar K^+ currents, with wild-type plants yielding mean steady-state values for $I_{K,in}$ at −240 mV and $I_{K,out}$ at +40 mV of -821 ± 35 μA cm^{-2} ($n = 15$) and $+183 \pm 13$ μA cm^{-2} ($n = 12$), respectively; guard cells of the *slac1-1* mutant, however, gave currents of -164 ± 37 μA cm^{-2} ($n = 14$) and $+295 \pm 22$ μA cm^{-2} ($n = 12$), corresponding to an 80% reduction and 61% increase at these voltages, respectively (Fig. 1, A and B; Table I). Additionally, the mean membrane voltage of *slac1-1* mutant guard cells was displaced negative relative to values recorded from guard cells of wild-type and *pSLAC1* Arabidopsis, consistent with the loss of inward current through the SLAC1 channel (Fig. 1C).

Thermodynamic considerations preclude the SLAC1 channel from contributing to anion uptake and stomatal opening (Blatt, 2000; Vahisalu et al., 2008; Barbier-Brygoo et al., 2011). Indeed, eliminating the SLAC1 current was expected to accelerate opening by eliminating an efflux shunt that opposed anion accumulation via H^+-coupled transport and might otherwise slow the accumulation of Cl^-. By contrast, $I_{K,in}$ is a dominant pathway for K^+ uptake during opening (Blatt, 2000; Hills et al., 2012); its suppression in the *slac1-1* mutant, therefore, was expected to slow stomatal opening. To monitor opening, we measured apertures from stomata in situ in leaves and after isolation in epidermal peels, and we recorded transpiration from intact Arabidopsis plants in response to step changes in light. Gas-exchange measurements (Fig. 2A) yielded rates of change in transpiration that were slowed significantly in the *slac1-1* mutant when compared with the wild-type and *pSLAC1* plants on transitions to light, and after isolation in epidermal peels, stomata of the *slac1-1* mutant opened in the light at roughly one-half the rate (Fig. 2A) and with half-times more than 2-fold greater than either the wild-type or *pSLAC1* plants (Fig. 2B). Over a 24-h period, stomata in leaves failed to close fully, opened and closed sluggishly, and responded over an elevated range of apertures in the *slac1-1* mutant when compared with the wild-type or *pSLAC1* plants (Fig. 2C), thus confirming the unexpected and ameliorating effect of the *slac1* mutation on water loss through slowed stomatal opening.

Altered K^+ Channel Activities Are Not Reflected in Channel Gene Transcription

The expression of several ion channel genes in Arabidopsis is subject to environmental cues and,

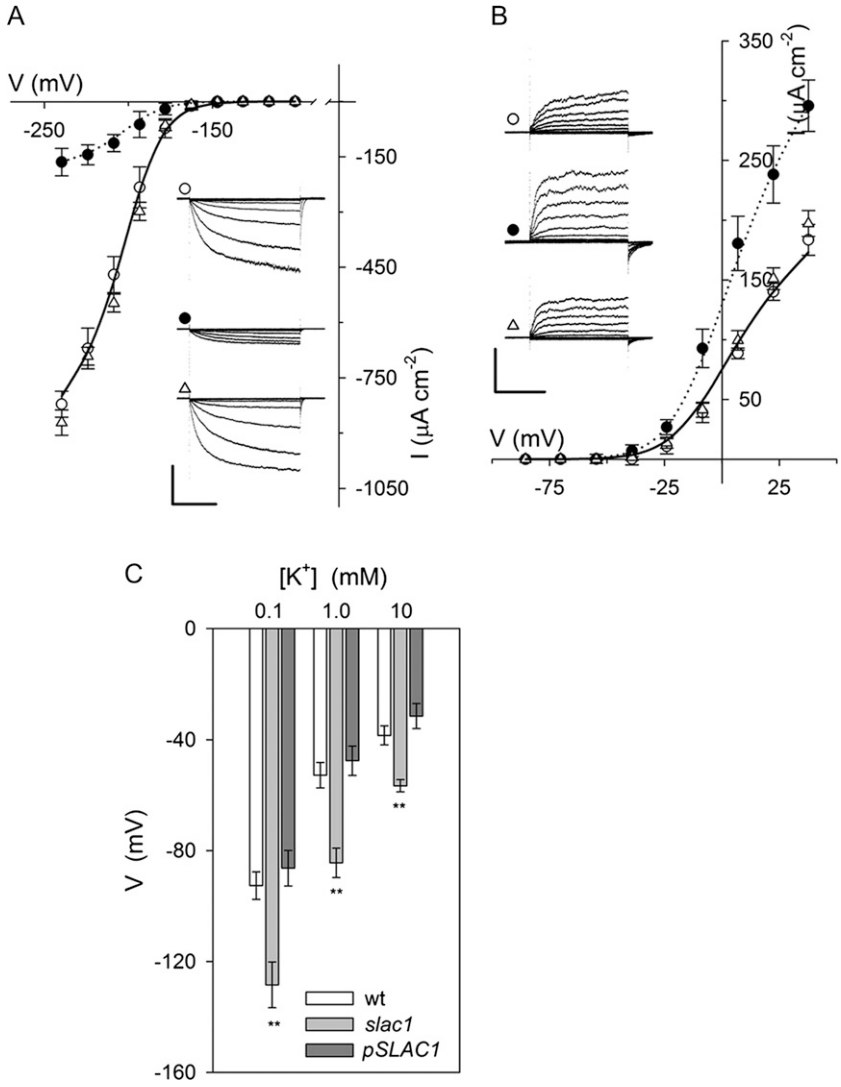

Figure 1. The *slac1* mutant of Arabidopsis alters currents carried by both $I_{K,in}$ and $I_{K,out}$ and hyperpolarizes the membrane voltage. Data are means ± SE of $n \geq 12$ independent experiments for wild-type (open circles), *slac1-1* (closed circles), and *pSLAC1* (open triangles) plants. A, Steady-state currents recorded under voltage clamp for $I_{K,in}$ show a roughly 80% suppression of channel current. Curves are fittings of wild-type (solid line) and *slac1-1* (dotted line) currents to a Boltzmann function (Table I). The inset shows current traces recorded under voltage clamp and cross referenced by symbol. Scale are as follows: vertical, 500 μA cm^{-2}; horizontal, 2 s. *slac1-1* currents are significantly different ($P < 0.001$) for all points negative of −180 mV. B, Steady-state currents recorded for $I_{K,out}$ under voltage clamp show a roughly 80% suppression of channel current. Curves are fittings of wild-type (solid line) and *slac1-1* (dotted line) currents to a Boltzmann function (Table I). The inset shows representative current traces recorded under voltage clamp and cross-referenced by symbol. Scale are as follows: vertical, 200 μA cm^{-2}; horizontal, 2 s. *slac1-1* currents are significantly different ($P < 0.001$) for all points positive of −20 mV. C, Free-running voltages recorded from wild-type (wt), *slac1-1*, and *pSLAC1* Arabidopsis with 0.1, 1, and 10 mM KCl outside. Values for the *slac1-1* mutant differ significantly (**$P < 0.001$) from those of wild-type and *pSLAC1* guard cells at all three KCl concentrations. Note that all values are likely to underestimate the true free-running voltage in this case, given the membrane input resistance (greater than 20 GΩ; Blatt and Slayman [1983]) and leakage currents (1–2 pA) typical of high-impedance electrometer amplifiers. Such leakage currents are insignificant as a background to clamp currents of ±300 to 500 pA, so they do not influence measurements under voltage clamp, but they are sufficient to displace the apparent voltage by +40 mV or more in the free-running (unclamped) cell.

potentially, to homeostatic regulation (Amtmann and Blatt, 2009). Therefore, we tested whether the *slac1-1* mutation might affect K^+ channel gene transcription. Transcripts for the K^+ channel genes *KAT1*, *KAT2*, *KC1*, *GORK*, *AKT1*, and *AKT2* were assayed by quantitative PCR using mRNA isolated from plants grown together and harvested 2 h after the start of daylight. We assayed for transcripts of the predominant vacuolar K^+ channel *TPK1* (Gobert et al., 2007) and the K^+- and Ca^{2+}-permeable channel *TPC1* (Peiter et al., 2005) as

Table I. *Fittings for $I_{K,in}$ and $I_{K,out}$ from Arabidopsis guard cells to a Boltzmann function (see Eq. 1)*

Fitted curves for wild-type and *slac1-1* currents are as shown (for details, see Figs. 1 and 6). Best fittings were obtained with the voltage sensitivity coefficient (gating charge; δ), held in common in both cases, and with the voltage yielding half-maximal conductance ($V_{1/2}$), held in common for $I_{K,out}$, as indicated. Note the roughly 80% reduction in maximum conductance (g_{max}) for $I_{K,in}$ and its 60% enhancement for $I_{K,out}$ in the *slac1-1* mutant.

Parameter	Wild Type	*slac1-1*	*pSLAC1*
$I_{K,in}$ (δ, -1.9 ± 0.1)			
g_{max} (μS cm^{-2})	4.83 ± 0.08	0.99 ± 0.07	5.20 ± 0.09
$V_{1/2}$ (mV)	-187 ± 3	-202 ± 2	-189 ± 2
$I_{K,out}$ (δ, 2.0 ± 0.1; $V_{1/2}$ -7 ± 2 mV)			
g_{max} (μS cm^{-2})	1.65 ± 0.07	2.83 ± 0.09	1.84 ± 0.08

well as for the vacuolar VH^+-ATPase C subunit *VHA-C* and the plasma membrane H^+-ATPases *AHA1*, *AHA2*, and *AHA5* that could affect energization of the membranes (Haruta and Sussman, 2012). No difference between the three plant lines was seen (Fig. 3), thus discounting homeostatic feedback via transcription.

slac1 Is Predicted to Elevate pH and $[Ca^{2+}]_i$, Affecting K^+ Channels and Stomatal Opening

To explore the physiological context of the *slac1-1* mutation, we next made use of quantitative systems modeling of the guard cell, incorporating all of the known transporters at the plasma membrane and tonoplast, their biophysical and kinetic characteristics, the salient features of Suc and Mal metabolism, as well as the homeostatic parameters of Ca^{2+} and pH buffering (Hills et al., 2012). We used an equivalent ensemble of model parameters (Chen et al., 2012b) to simulate the diurnal cycle of stomatal movements after scaling guard cell volume and stomatal aperture to the dimensions of the Arabidopsis stomatal complex while maintaining transporter surface densities (Supplemental Appendix S1). An essential feature of this modeling approach is that the system is defined by a set of model components (transporters and metabolic and buffering reactions), the parameters of which are fixed constants defined experimentally. Thus, all of the dynamic behavior of the system arises from the emergent interactions between model components and associated dependent variables, notably of ion and solute concentrations, and of the voltages across the two membranes (Chen et al., 2012b). Simulations were carried out first with the full complement of membrane transporters, including the SLAC1 current, and then with the SLAC1 current omitted. The model reproduced the behavior of the wild-type Arabidopsis stomata and all of the salient features of the *slac1-1* mutant, notably the elevated range of stomatal

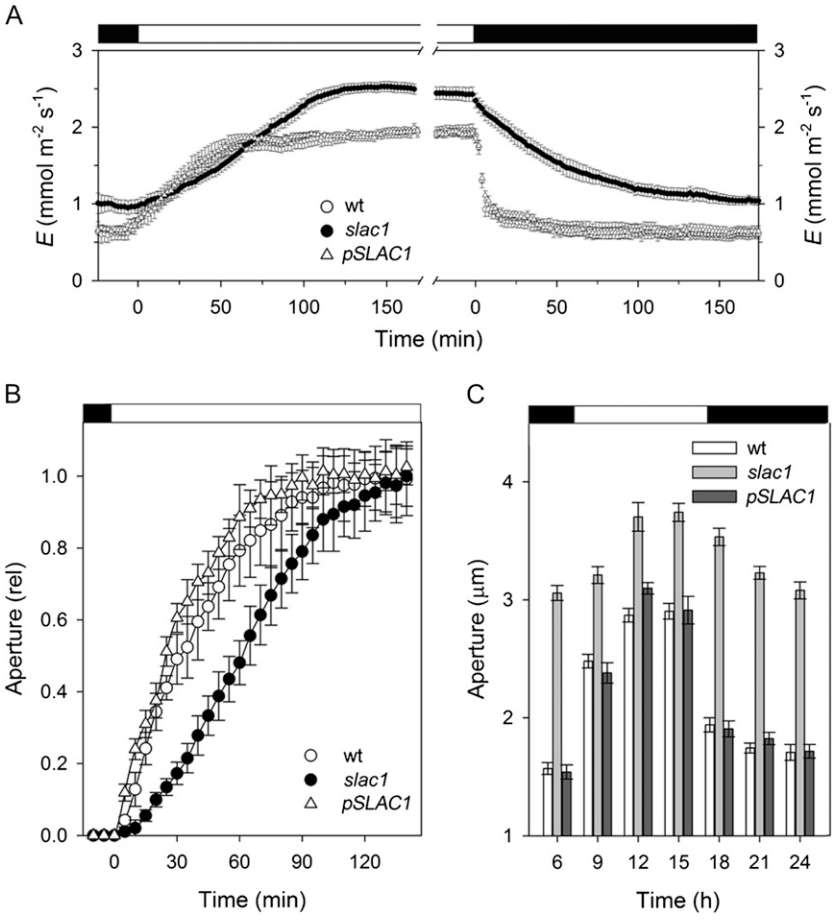

Figure 2. The *slac1* mutant of Arabidopsis slows stomatal opening and closing on light-dark transitions. Data are means $\pm$ SE of $n \geq 12$ independent experiments for wild-type (wt; open circles), *slac1-1* (closed circles), and *pSLAC1* (open triangles) plants. A, Transpiration rates recorded from intact Arabidopsis on transition from dark to 300 μmol m^{-2} s^{-1} light (left) and back to dark (right). Fitted half-times for opening (sigmoid) and closing (single exponential) are as follows: wild type, 22.4 ± 0.5 and 5.5 ± 0.2 min; *slac1-1*, 65.6 ± 0.4 and 50.7 ± 0.4 min; *pSLAC1*, 27.1 ± 0.4 and 6.3 ± 0.1 min. B, Stomatal apertures from epidermal peels. Data are normalized to initial and final apertures on transition to 300 μmol m^{-2} s^{-1} light. Opening half-times are as follows: wild type, 38 ± 5 min; *slac1-1*, 74 ± 8 min; *pSLAC1*, 34 ± 7 min. Apertures (initial/final, in μm) are as follows: wild type, $2.6 \pm 0.2/4.2 \pm 0.4$; *slac1-1*, $4.0 \pm 0.3/4.8 \pm 0.4$; *pSLAC1*, $2.6 \pm 0.2/4.0 \pm 0.4$. C, Stomatal opening and closing recorded in leaves at 3-h intervals over 24 h. Note the slower response in the first three daylight hours for the mutant. *slac1-1* apertures are significantly different ($P < 0.001$) at all times.

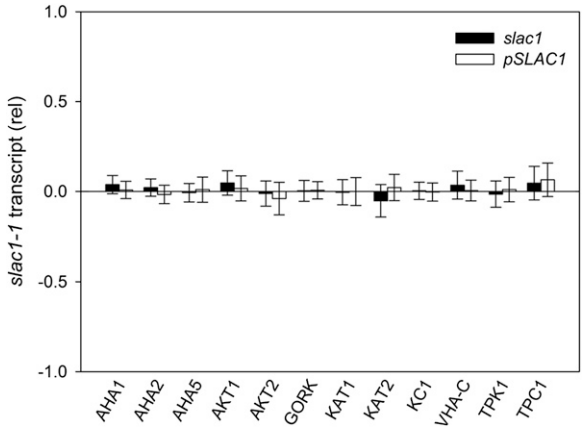

Figure 3. Relative transcript levels for selected plasma membrane and tonoplast transporters from *slac1-1* and *pSLAC1* Arabidopsis assayed by quantitative PCR. Data are means ± SE of three independent experiments and are reported as the change in expression relative to wild-type levels (=0) after normalizing to the housekeeping *ACT2* actin gene and *TUB9* tubulin gene transcripts.

apertures and accumulation of Cl^-, Mal, and K^+ (Fig. 4A); it returned roughly a 5-fold increase in the half-time for closure and a slowed rate of stomatal opening (Fig. 4B); and it enhanced $I_{K,out}$ and greatly reduced $I_{K,in}$ activities in the *slac1-1* simulation (Fig. 4, C and D), much as observed experimentally (Figs. 1 and 2).

The model also yielded two key predictions for the *slac1-1* mutant: (1) it showed roughly a 0.2-unit elevation in pH_i above the means in the wild type, day and night; and (2) it predicted a rise in the daytime $[Ca^{2+}]_i$, to values near 400 nM (Fig. 4E). Significantly, both elevated pH_i and $[Ca^{2+}]_i$ are known to suppress $I_{K,in}$. In *Vicia faba* guard cells, $[Ca^{2+}]_i$ inactivates $I_{K,in}$ with an inhibitory constant, k_i of 330 nM and a Hill coefficient of 4 (Grabov and Blatt 1999), and the current activates with cytosolic protein concentration $[H^+]_i$ (decreasing pH_i), showing an apparent $K_{1/2}$ near 400 nM (pH 6.4) and Hill coefficient of unity (Blatt, 1992; Grabov and Blatt, 1997). Raising pH_i also enhances $I_{K,out}$, the current exhibiting a K_i for H^+ near 40 nM (pH 7.4) and a Hill coefficient of 2 (Blatt and Armstrong, 1993; Grabov and Blatt, 1997). Such quantitative detail is not available for the guard cells of Arabidopsis, but all evidence (Hoth and Hedrich, 1999; Hosy et al., 2003; Siegel et al., 2009) indicates similar pH_i and $[Ca^{2+}]_i$ sensitivities. Thus, we suspected that the elevations in pH_i and $[Ca^{2+}]_i$ predicted for the *slac1-1* guard cells might explain the altered K^+ currents of the mutant.

Direct pH and $[Ca^{2+}]_i$ Measurements and Manipulations Validate Model Predictions

To test these predictions, we recorded pH_i and $[Ca^{2+}]_i$ in vivo by ratiometric fluorescence imaging using the H^+-sensitive dye 2′,7′-bis-(2-carboxyethyl)-5,(6)-carboxyfluorescein (BCECF) and the Ca^{2+}-sensitive dye 2-(6-(bis(carboxymethyl)amino)-5-(2-(2-(bis(carboxymethyl)amino)-5-methylphenoxy)ethoxy)-2-benzofuranyl)-5-oxazolecarboxylic acid (Fura2) after iontophoretic injection into guard cells. Recordings of BCECF fluorescence yielded pH_i near 7.6 in wild-type and *pSLAC1* guard cells, similar to guard cells of *V. faba* (Blatt and Armstrong, 1993; Grabov and Blatt, 1997). Recordings from *slac1-1* guard cells showed an elevated pH_i (Fig. 5A), consistent with, and even exceeding, model predictions. We used treatments with butyrate to acid load the cytosol and to calculate the H^+ buffering capacity of the guard cells, much as we have before (Blatt and Armstrong, 1993; Grabov and Blatt, 1997). When protonated, the organic acid is freely permeable across the plasma membrane and sets up coupled dissociation equilibria according to the Henderson-Hasselbalch equation and determined by the dominant pool of protonated acid. For a cell, the near-infinite volume of bathing solution determines the protonated acid concentration. Thus, equilibration of the protonated acid across the plasma membrane and its dissociation generates a substantial cytosolic H^+ load, provided that the bath is 1 to 2 pH units more acidic than the cytosol (McLaughlin and Dilger, 1980). Butyrate treatments carried out while measuring pH_i with BCECF showed a significant acidification of the cytosol (Fig. 5B). From the Henderson-Hasselbalch equation, we calculated a cytosolic buffer capacity of 84 ± 6 mM H^+ per pH unit for guard cells of wild-type Arabidopsis, close to that for *V. faba* guard cells (Grabov and Blatt, 1997), and almost a 2-fold higher buffer capacity of 143 ± 13 mM per pH unit in the *slac1-1* mutant (Fig. 5A). The elevated pH_i buffer capacity of *slac1-1* guard cells is consistent with the substantial retention of organic acids reported previously (Negi et al., 2008). Measurements of $[Ca^{2+}]_i$ with Fura2 from guard cells of wild-type and *pSLAC1* plants gave resting values near 220 nM, whereas *slac1-1* guard cells showed significantly elevated $[Ca^{2+}]_i$, with a mean value near 450 nM (Fig. 5C). Thus, in *slac1-1* guard cells, the elevations in pH_i and $[Ca^{2+}]_i$ alone appeared sufficient to explain both $I_{K,in}$ suppression and the enhancement of $I_{K,out}$, assuming kinetic sensitivities similar to those for the K^+ channels in *V. faba.*

To validate this conclusion, we tested the capacity to recover wild-type $I_{K,in}$ and $I_{K,out}$ in the *slac1-1* mutant when $[Ca^{2+}]_i$ and pH_i were chemically "clamped" to suppress their elevation. Guard cells of the *slac1-1* mutant were impaled as before, but with electrolyte including 10 mM of the Ca^{2+} buffer 1,2-bis(2-aminophenoxy) ethane-*N*,*N*,*N*′,*N*′-tetraacetic acid (BAPTA; K_d = 130 nM) for direct loading from the microelectrode. Loading with Ca^{2+} buffers has been used on many occasions to lower resting $[Ca^{2+}]_i$ and to suppress $[Ca^{2+}]_i$ transients (Speksnijder et al., 1989; Fairley-Grenot and Assmann, 1991; Felle and Hepler, 1997). In our experience, BAPTA loading in guard cells effectively clamps $[Ca^{2+}]_i$ near 200 nM, even under conditions that normally drive $[Ca^{2+}]_i$ above 1,200 nM (Chen et al., 2010). Following impalements and BAPTA loading, the guard cells were challenged with 3 mM

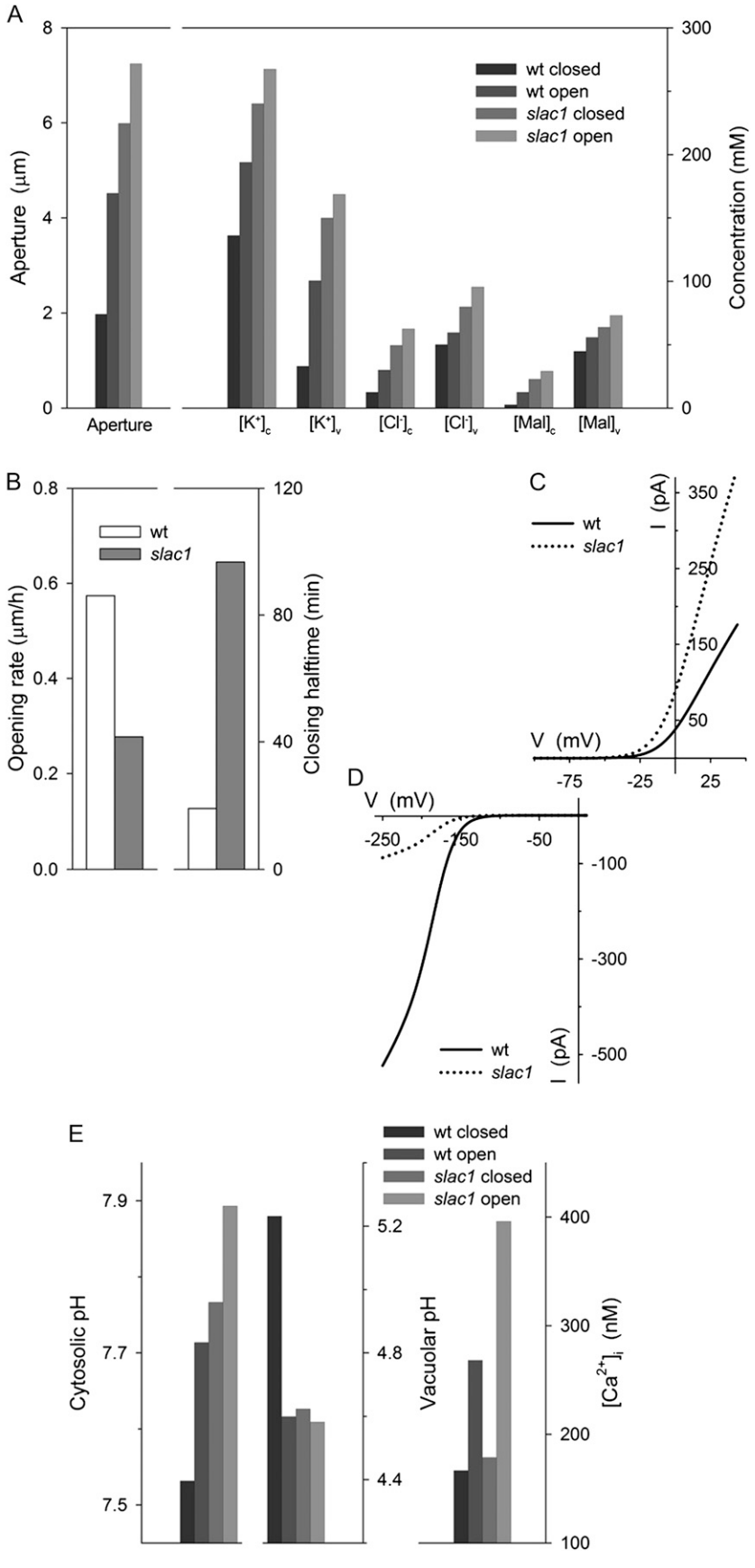

Figure 4. Quantitative systems modeling (Chen et al., 2012b; Hills et al., 2012) reproduces characteristics for *slac1-1* guard cells and accounts for altered K^+ channel activities through predicted elevations of pH_i and $[Ca^{2+}]_i$. Outputs are derived from modeling of the diurnal cycle (Chen et al., 2012b). Additional model outputs and detailed explanations are provided with Supplemental Figures S1 to S7. The full set of model parameters and initializing variables are listed in Supplemental Appendix S1 and are available with the OnGuard software at www.psrg.org.uk. A, Mean stomatal apertures and cytosolic and vacuolar solute concentrations for guard cells of stomata in the dark (closed) and light (open). Outputs are for each variable (left to right, wild-type [wt] closed and open, *slac1* closed and open). B, Stomatal opening rates (left) and closure half-times (right) determined from simulated apertures during the first 3 h (opening) and the final 3 h (closing) of the daylight period (compare with Fig. 2; Supplemental Fig. S1). C and D, Current-voltage curves for $I_{K,out}$ (C) and $I_{K,in}$ (D) in wild-type (solid line) and *slac1* (dotted line) simulations taken at 3 h into the daylight period (compare with Fig. 1, A and B). E, Predicted outputs (left to right, outputs for wild-type closed and open, *slac1* closed and open) for pH_i (left), vacuolar pH (center), and $[Ca^{2+}]_i$ (right).

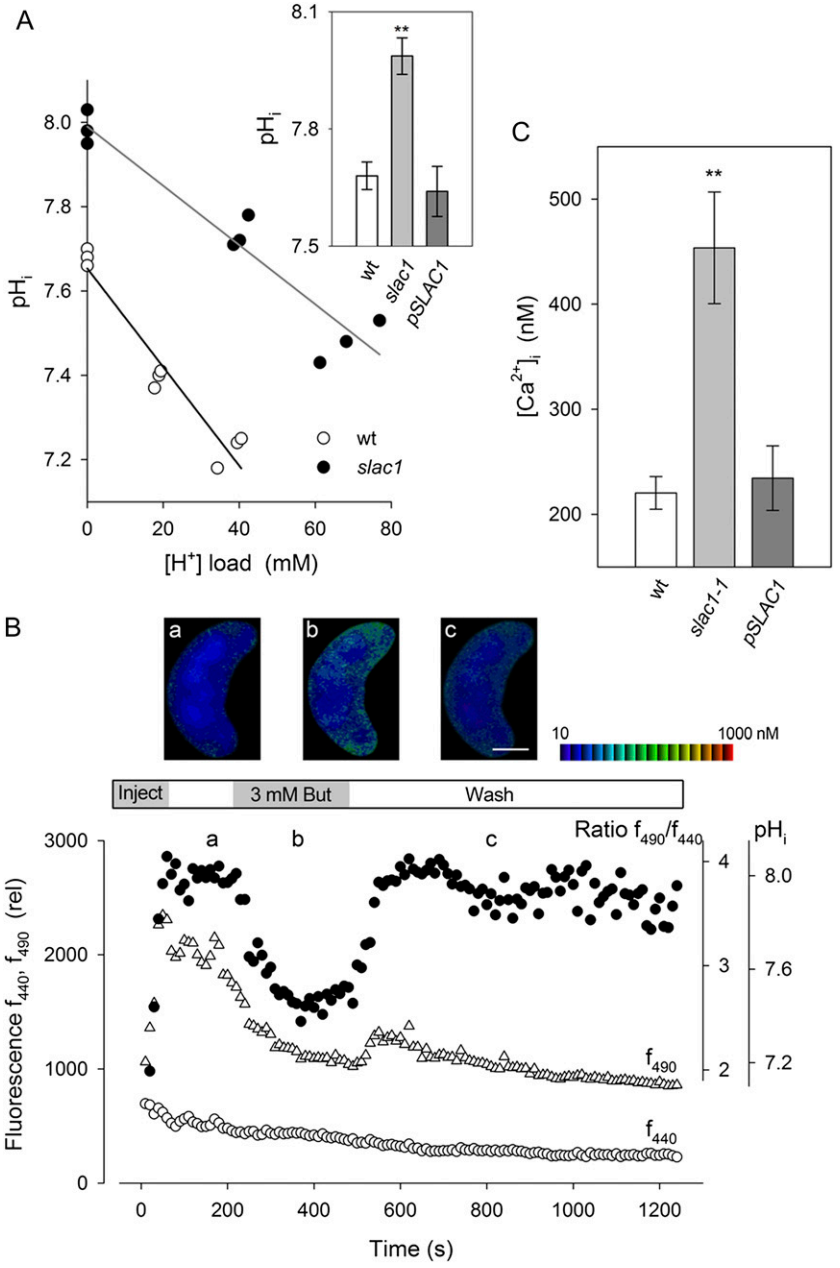

Figure 5. The *slac1-1* mutant shows elevated pH_i and $[Ca^{2+}]_i$. A, Mean ± SE for pH_i (inset; $n \geq 7$) and pH buffering analysis ($n = 3$) from guard cells of wild-type (wt; open circles) and *slac1-1* mutant (closed circles) Arabidopsis using BCECF fluorescence ratio analysis and before and during acid loading with 1 and 3 mM butyrate. Buffering determined by linear fitting (solid lines; Grabov and Blatt 1997) gave 84 ± 6 mM H^+ per pH unit (wild type) and 143 ± 13 mM per pH unit (*slac1-1*). pH_i values from *slac1-1* guard cells differed significantly (**$P < 0.001$) from those of wild-type and *pSLAC1* plants. B, pH_i recording from one *slac1-1* mutant guard cell using BCECF fluorescence ratiometry. Fluorescence at 440 nm (f_{440}; open circles), 490 nm (f_{490}; open triangles), and the fluorescence ratio (f_{490}/f_{440} and calibrated pH_i; closed circles) were recorded at 10-s intervals from 1.5 μm depth around the cell periphery. Representative images (top) were taken at the time points indicated. The intensity-modulated pseudocolor scale (left to right) represents pH 8 to 6. The period of BCECF injection, exposure to 3 mM butyrate (But), and butyrate washout are as indicated. C, Mean ± SE ($n \geq 5$) for resting $[Ca^{2+}]_i$. Values for *slac1-1* guard cells differed significantly (**$P < 0.001$) from those of the wild type and *pSLAC1*.

butyrate to lower pH_i near a value of 7.5, close to that of wild-type guard cells (Fig. 5, A and B). Analysis of five independent experiments with *slac1-1* guard cells (Fig. 6, A and B) showed that these manipulations were sufficient to recover both $I_{K,in}$ and $I_{K,out}$ in the *slac1-1* mutant, with characteristics that were quantitatively equivalent to those observed in the wild-type plant. We used a similar strategy in measurements of stomatal opening. Buffering $[Ca^{2+}]_i$ by BAPTA loading was not possible in this case, so guard cells in epidermal peels were treated with butyrate to suppress pH_i as before. The results yielded rates of stomatal opening statistically equivalent to those of wild-type guard cells (Fig. 6C), consistent with evidence that greater than 70% suppression of $I_{K,in}$ is necessary before a significant change in opening or its kinetics is measurable (Lebaudy et al., 2008).

DISCUSSION

The detail now available for, and complexity of, guard cell transport defy any simple explanation for how guard cells achieve the range of stomatal apertures observed in vivo, let alone a clear understanding of the properties of the guard cell system as a whole. This gap in understanding is evident especially in the counterintuitive behavior of stomata of the *slac1* mutant of Arabidopsis. *slac1* guard cells lack the major anion channel that mediates anion efflux during stomatal closure; yet paradoxically, the cells show

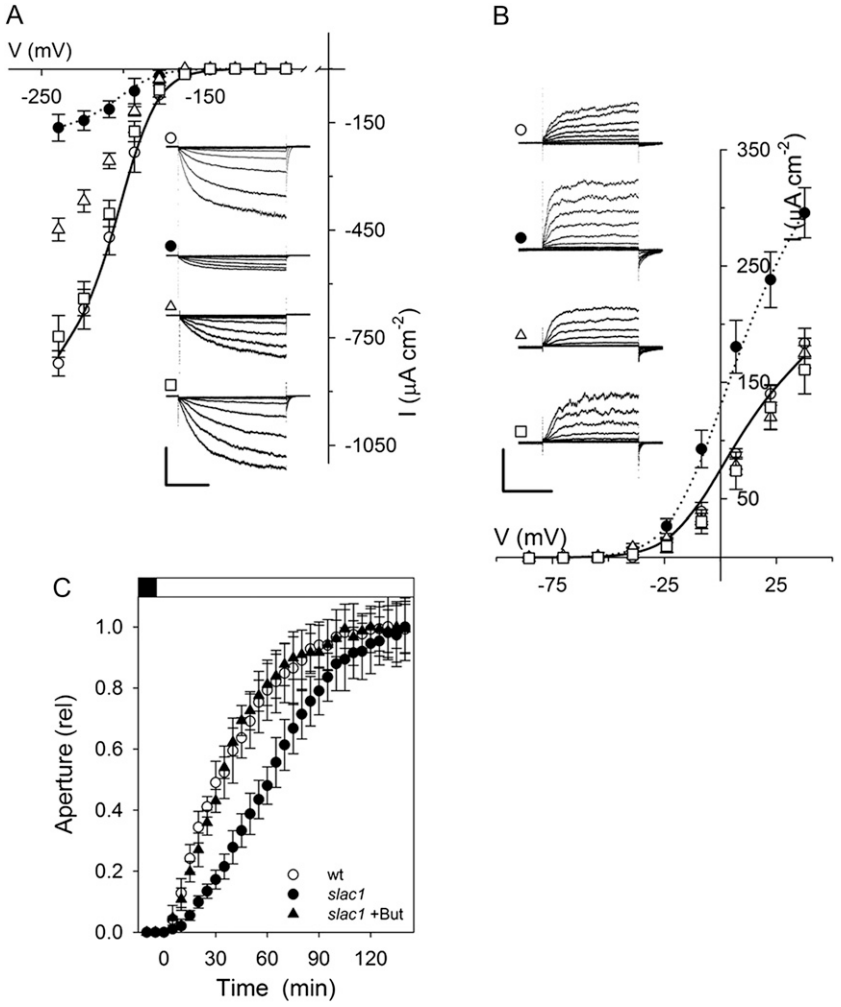

Figure 6. Altered K^+ channel currents are consequent on elevation of pH_i and $[Ca^{2+}]_i$ in the *slac1-1* mutant. A, Mean ± SE ($n \geq 8$) of steady-state currents for $I_{K,in}$ under voltage clamp show recovery of wild-type characteristics in the *slac1-1* mutant on suppressing $[Ca^{2+}]_i$ and pH_i elevations. Wild-type (open circles) and *slac1-1* (closed circles) data are included from Figure 1 for reference. *slac1-1* guard cells were loaded with 10 mM BAPTA to buffer $[Ca^{2+}]_i$ (open triangles) and additionally exposed to 3 mM butyrate outside (open squares) to lower pH_i (Fig. 5, A and B). The inset shows current traces recorded under voltage clamp and cross-referenced by symbol. Scales are as follows: vertical, 500 μA cm^{-2}; horizontal, 2 s. B, Mean ± SE ($n \geq 7$) of steady-state currents for $I_{K,out}$ under voltage clamp show recovery of wild-type current characteristics in *slac1-1* mutant guard cells on suppressing pH_i elevation. Wild-type (open circles) and *slac1-1* (closed circles) data are included from Figure 1 for reference. *slac1-1* guard cells were exposed to 3 mM butyrate outside (open squares) to lower pH_i (Fig. 5, A and B) and additionally when loaded with 10 mM BAPTA to buffer $[Ca^{2+}]_i$ (open triangles). The inset shows current traces recorded under voltage clamp and cross referenced by symbol. Scales are as follows: vertical, 200 μA cm^{-2}; horizontal, 2 s. C, Stomatal opening in epidermal peels on transition to 300 μmol m^{-2} s^{-1} light in the presence of 3 mM butyrate (But). Data are normalized to initial and final apertures after correcting for butyrate-induced aperture increase. Results for the wild type (wt) and the *slac1-1* mutant are included from Figure 1 for comparison. Opening half-time was as follows: *slac1-1* + butyrate, 23 ± 0.8 min. Apertures (initial/final in μm) are as follows: wild type, 2.7 ± 0.3/4.5 ± 0.3; *slac1-1*, 4.3 ± 0.3/5.1 ± 0.3; *slac1-1* + butyrate, 4.5 ± 0.2/5.6 ± 0.2.

profound changes in K^+ channel activities and a slowed rate of stomatal opening. We have taken a computational approach to quantitative dynamic modeling of the guard cell to understand this behavior. The model incorporates all of the properties for transporters at the plasma membrane and tonoplast, the salient features of osmolite metabolism, and pH and Ca^{2+} buffering. The results demonstrate the true predictive power of this systems modeling approach to guide a detailed mechanistic analysis of the signaling pathways responsible. Furthermore, in so doing, they highlight a previously unrecognized homeostatic network that regulates membrane transport for stomatal function. The SLAC1 channel has no direct connection with solute uptake, and especially not with $I_{K,in}$ and K^+ influx; however, modeling uncovered the feedback

pathway to the K^+ channels, and we confirmed experimentally the link through the effect of *slac1* in elevating pH_i and $[Ca^{2+}]_i$ (Fig. 7). This network ameliorates the effect of the *slac1* mutation by suppressing $I_{K,in}$ and the rise in transpiration during the first hours of daylight, thus explaining the otherwise counterintuitive effects of *slac1* on stomatal movement.

In the model, just as in vivo, changes in $[Ca^{2+}]_i$ and pH_i arise through interactions between the various transporters, metabolism, and associated buffering characteristics (Chen et al., 2012b; Hills et al., 2012). The model accounts for the emergent effects of the *slac1* mutant on pH_i as a consequence of Cl^- and Mal hyperaccumulation, much as has been observed in vivo (Negi et al., 2008). A detailed analysis of the model outputs is presented in Supplemental Figures S1 to S7. It predicted pH_i in the mutant to rise with Mal transinhibition of Mal synthesis and of Cl^- -mediated transinhibition of H^+-coupled anion transport. Strongly affected was the H^+-Cl^- antiport at the tonoplast, which normally transports inorganic anions into the vacuole in exchange for H^+ (De Angeli et al., 2006;

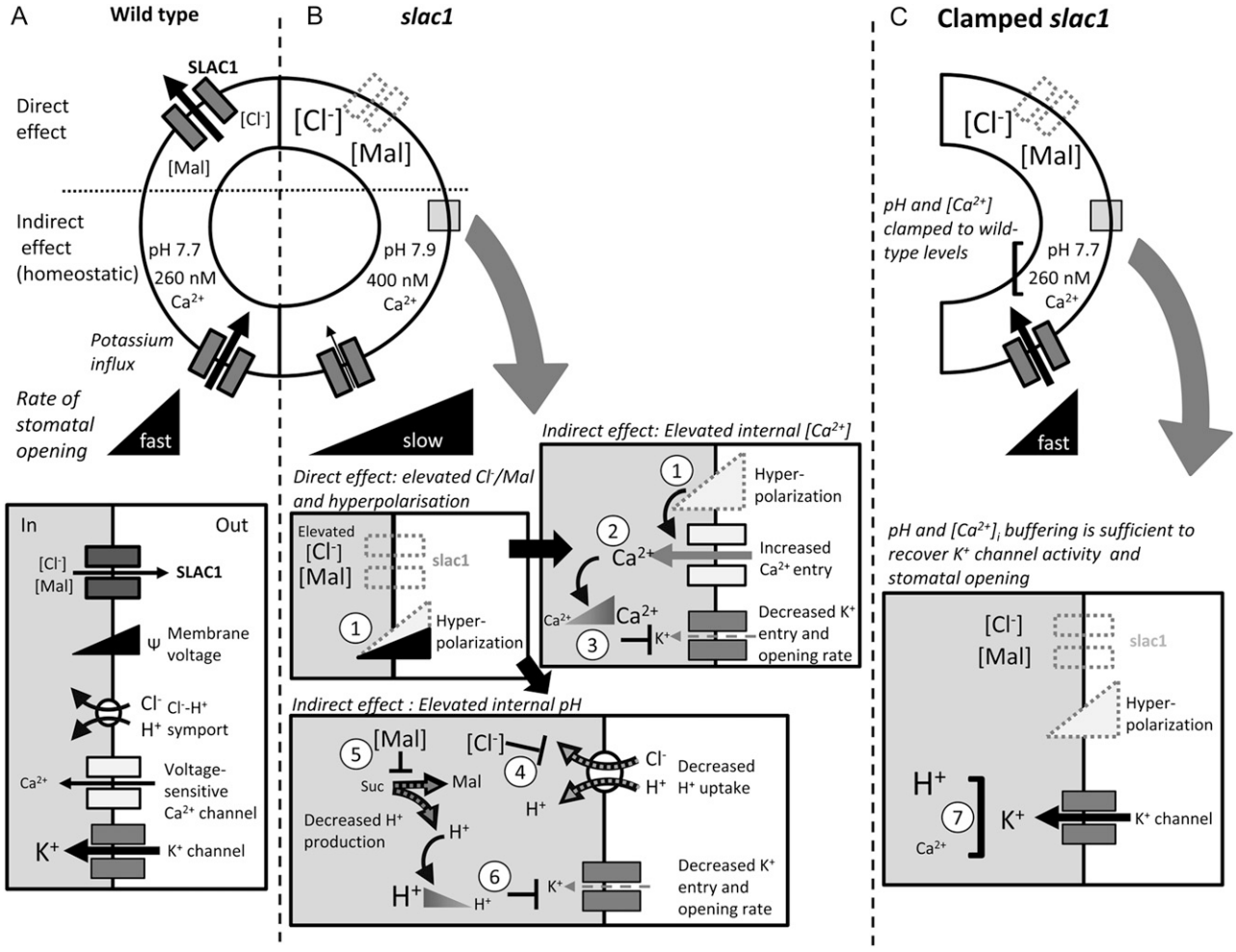

Figure 7. Eliminating the SLAC1 anion channel affects K^+ channel activity, K^+ uptake, and the rate of stomatal opening through its impact on pH_i and $[Ca^{2+}]_i$ as predicted by the OnGuard model (Chen et al., 2012b; Hills et al., 2012). Note that effects on tonoplast transport and on $I_{K,out}$ are not included for clarity, but they are complementary (see text). Black arrows indicate the wild type, and gray arrows indicate *slac1*. A, SLAC1 is a major pathway for Cl^- efflux during stomatal closure and is facilitated when Ca^{2+} channels activate to raise $[Ca^{2+}]_i$. The K^+ channel ($I_{K,in}$) and H^+-coupled Cl^- transport enable osmotic solute uptake during opening. B, The *slac1* mutation eliminates an inward current (anion efflux), leading directly to Cl^- and Mal accumulation and membrane hyperpolarization (1) in the guard cell (Supplemental Figs. S1–S3). Membrane hyperpolarization promotes Ca^{2+} entry by activating plasma membrane Ca^{2+} channels (2) and elevates $[Ca^{2+}]_i$ (Fig. 5; Supplemental Fig. S6), which in turn suppresses $I_{K,in}$ (3; Fig. 1; Supplemental Fig. S7). Elevated Cl^- and Mal suppress H^+-coupled Cl^- transport (4; see Supplemental Fig. S2) and Mal synthesis (5; Supplemental Fig. S3), thereby reducing the H^+ load on the cytosol and raising pH_i (Supplemental Fig. S5). The rise in pH_i also suppresses $I_{K,in}$ (6). The predicted increases in $[Ca^{2+}]_i$, pH_i, and their consequences for the K^+ channels were confirmed experimentally (Figs. 5 and 6). C, Suppressing the rise in $[Ca^{2+}]_i$ and pH_i by buffering (7) was sufficient to recover K^+ channel activity and the rate of stomatal opening, thus validating the model (Fig. 6).

Jossier et al., 2010). Overall, the result was to reduce the metabolic and transport H^+ load on the cytosol, including H^+ return to balance the H^+-ATPase at the plasma membrane (Supplemental Fig. S5), hence raising pH_i. Thus, one important conclusion to be drawn from this first of the model predictions, and from its experimental validation, is of the central importance played by H^+-coupled anion transport in controlling pH_i. A detailed knowledge of Cl^- uptake in plants is restricted to a few cell types (Sanders et al., 1989), but, like that of NO_3^- (Meharg and Blatt 1995), it is generally recognized to be mediated in symport with H^+. In fact, H^+-coupled anion transport at both membranes has been suggested to contribute to pH_i homeostasis (Barbier-Brygoo et al., 2011; Chen et al., 2012b), although direct and quantitative evidence has been lacking until now.

The model ascribes the elevated $[Ca^{2+}]_i$ of the mutant to loss of the SLAC1-mediated (inward) current and consequent negative shift in membrane voltage, thus promoting Ca^{2+} entry across the plasma membrane (Fig. 1; Supplemental Figs. S1 and S6). By contrast with the situation for pH_i, the effect of membrane hyperpolarization in promoting Ca^{2+} influx and elevating $[Ca^{2+}]_i$ in guard cells is well documented (Grabov and Blatt, 1998, 1999; Hamilton et al., 2000; Chen et al., 2010). We note that Vahisalu et al. (2008) reported little difference in $[Ca^{2+}]_i$ between wild-type and *slac1* mutant guard cells when recorded using the Cameleon YC3.6 Ca^{2+}-sensitive reporter. However, their measurements were determined under experimental conditions known to drive $[Ca^{2+}]_i$, indeed, via control of membrane voltage (Grabov and Blatt, 1998, 1999; Allen et al., 2001), effectively clamping $[Ca^{2+}]_i$ either to high or low values. Thus, their measurements cannot speak to the free-running $[Ca^{2+}]_i$, either in the wild-type or *slac1* mutant guard cells.

We stress that our results uncover a homeostatic signaling network that, in itself, is sufficient to explain the physiopathology of the *slac1* mutant and its phenotypic characteristics in altered K^+ transport and stomatal opening. These findings do not rule out other consequences of the *slac1* mutation, such as might be effected through more subtle changes in pH_i or $[Ca^{2+}]_i$ sensitivities of one or more of the underlying channels; however, they demonstrate that any such changes are not, in themselves, essential to understanding the effect of the *slac1* mutant either on K^+ channel activities or on stomatal movement. Our findings also pave the way, through similar dynamic modeling and validation, to addressing many other unresolved observations in stomatal physiology. This strategy is certain to yield a greater understanding of the impacts of transport at the plasma membrane. Furthermore, it should prove a powerful new tool with which to analyze transport at the tonoplast, for which direct access in vivo is not possible. Challenges, for example, include resolving the controversial roles for the TPC1 cation channel in stimulus-response coupling (Peiter et al., 2005) and the counterintuitive effects of the TPK1 K^+ channel and CLCc anion antiporter, the deletion of either of which slows stomatal closure but with counterintuitive effects on K^+ (Gobert et al., 2007) and anion content (Jossier et al., 2010). Analysis of these problems will help refine our current model of the guard cell as well as our understanding of stomatal function.

MATERIALS AND METHODS

Growth and Whole-Plant Physiology

Arabidopsis (*Arabidopsis thaliana*) Columbia wild-type, *slac1-1* mutant, and *pSLAC1*-complemented *slac1-1* plants were grown under 70 μmol m^{-2} s^{-1} light in short-day conditions (8/16 h of light/dark) at 22°C/18°C and 55%/70% relative humidity. All seeds were harvested at the same time from plants grown together. Chemicals were reagent grade from Sigma-Aldrich. Gas exchange was measured using the LI-COR 6400 XT Infrared Gas Analyzer (LI-COR Biosciences) and Arabidopsis Chamber (LI-COR 6400-17). Pots were sealed with Saran Wrap to prevent water vapor and CO_2 diffusion from the soil, and measurements were carried out at 380 μL L^{-1} CO_2. Gas exchange was recorded in plants adapted to the dark for 2 h with light from an integrated source (LI-COR 6400-18). All plants were analyzed on at least 3 d at the same time of the relative diurnal cycle and were normalized for leaf area using ImageJ, version 1.43 (rsbweb.nih.gov/ij/; Rasband and Bright 1995).

Gene Expression Analysis

Total RNA was extracted from mature leaves, and transcript levels were determined by quantitative PCR as before (Chen et al., 2012b). Unique primers (Supplemental Table S1) were designed for the VH^+-ATPase C subunit (Dettmer et al., 2006), the plasma membrane H^+-ATPases *AHA1*, *AHA2*, and *AHA5* (Lopez-Marques et al., 2004), the K^+ channels *KAT1*, *KAT2*, *KC1*, *GORK*, *AKT1*, and *AKT2* (Pilot et al., 2001; Hosy et al., 2003; Honsbein et al., 2009), and the vacuolar channels *TPK1* (Gobert et al., 2007) and *TPC1* (Peiter et al., 2005). The *TUB9* tubulin (At4g20890) and *ACT2* actin (At3g18780) genes (Gutierrez et al., 2008) served as internal controls.

Stomatal Assays and Guard Cell Electrophysiology

Stomatal apertures in leaves were determined from impressions made using nail varnish and after peeling at intervals over 24 h (Fig. 2C). Otherwise, guard cells were isolated in epidermal peels and mounted as before (Eisenach et al., 2012). Stomatal apertures were recorded by digital photomicrography under infrared light (greate than 800 nm) and continuous superfusion with 10 mM KCl in 5 mM Ca^{2+}-MES buffer, pH 6.1 [5 mM MES buffer titrated to its acid dissociation constant with $Ca(OH)_2$; Ca^{2+} concentration = 1 mM]. Light treatments were carried out on dark-adapted peels.

Currents from intact guard cells were recorded under voltage clamp using double- and triple-barreled microelectrodes and Henry's EP suite (Y-Science; Blatt and Armstrong, 1993; Eisenach et al., 2012). Microelectrodes were pulled to give tip resistances greater than 500 MΩ for impalement of Arabidopsis guard cells, and microelectrode barrels were filled with 200 mM K^+ acetate, pH 7.5, to avoid Cl^- leakage from the microelectrode (Blatt and Slayman, 1983; Blatt, 1987b; Chen et al., 2012a). Voltage was recorded using a μP electrometer amplifier (WyeScience) with an input impedance of greater than 500 GΩ (Blatt, 1987a) and was typically clamped in cycles with a holding voltage of −100 mV and 6-s steps either to voltages from −120 to −240 mV ($I_{K,in}$) or to voltages from −80 to +40 mV ($I_{K,out}$). The Ca^{2+} buffer BAPTA was included as indicated. $[Ca^{2+}]_i$ and pH_i were determined, as described previously (Grabov and Blatt, 1997; Garcia-Mata et al., 2003), after iontophoretic injection of the fluorescent dyes Fura2 and BCECF, respectively. Fluorescence ratio imaging made use of a GenIV-intensified Pentamax CCD camera and TILL Polychrome II monochromator (Till Photonics), with excitation at 340 and 390 nm for $[Ca^{2+}]_i$ and 440 and 490 nm for pH_i. Fluorescence was collected after passage through a 535- ± 20-nm bandpass filter and was corrected for background before loading. Dye loading was judged successful by visual checks for cytosolic dye distribution and by stabilization of the fluorescence signals (Grabov and Blatt, 1997; Garcia-Mata et al., 2003). Image analysis was carried out using MetaFluor and MetaMorph (version 6.3; Universal Imaging), and measurements were calibrated in vitro and in vivo after permeabilization (Grabov and Blatt,

1997). Surface areas of impaled guard cells were calculated assuming a spheroid geometry. Subsequent data analysis and curve fittings were carried out using Henry's EP suite and SigmaPlot 11 (Systat Software). Measurements in the guard cells were validated by acid loading with the weak acid butyrate and by raising $[Ca^{2+}]_i$ on exposures to high external Ca^{2+} concentration (Allen et al., 2001).

Current-voltage analysis and fittings were carried out using Henry's EP suite and SigmaPlot 11 (Systat Software). Currents were fitted by joint, nonlinear least squares using a Boltzmann function of the form

$$I = \frac{g_{max}(V - E_K)}{1 + e^{\delta F(V_{1/2} - V)/RT}} \quad (1)$$

where δ is the voltage sensitivity coefficient (gating charge), E_K is the K^+ equilibrium voltage, g_{max} is the maximum conductance of the ensemble of channels, $V_{1/2}$ is the voltage yielding half-maximal activation, F is the Faraday constant, R is the universal gas constant, and T is the absolute temperature. Results are reported as means ± SE of n observations, with significances tested using Student's t test and ANOVA. As appropriate, significance was also verified by multiple pairwise comparisons (Student-Neumann-Keuls method) at $P < 0.05$ unless otherwise indicated.

OnGuard Modeling

The OnGuard software and model was driven through a diurnal 12/12-h light/dark cycle as described previously (Chen et al., 2012b), and all model outputs were derived from this cycle. Model parameters (Hills et al., 2012) were adjusted to reflect the physical dimensions of the Arabidopsis stomatal complex, and transporter numbers were scaled accordingly. Light sensitivity was assigned solely to the plasma membrane H^+-ATPase and Ca^{2+}-ATPase, the vacuolar VH^+-ATPase, H^+-pyrophosphatase, and Ca^{2+}-ATPase, and Suc synthesis in accordance with experimental observation (Chen et al., 2012b). All other model parameters were fixed, the properties of the individual transporters and buffering reactions thus responding only to changes in model variables arising from the kinetic features encoded in the model. The complete parameter set used to initiate modeling is provided in Supplemental Appendix S1, and the OnGuard software is available at www.psrg.org.uk.

Supplemental Data

The following materials are available in the online version of this article.

Supplemental Figure S1. Macroscopic outputs from the OnGuard model.

Supplemental Figure S2. Chloride contents and analysis of Cl^- fluxes at the plasma membrane and tonoplast.

Supplemental Figure S3. Malic acid synthesis, total malate contents, and analysis of Mal fluxes at the plasma membrane and tonoplast.

Supplemental Figure S4. Cytosolic and vacuolar pH, and analysis of H^+ fluxes across the plasma membrane and tonoplast.

Supplemental Figure S5. Total H^+ distribution summed over a 24-h period.

Supplemental Figure S6. Total cytosolic and vacuolar Ca^{2+} concentration, $[Ca^{2+}]_i$, and analysis of Ca^{2+} fluxes across the plasma membrane and tonoplast.

Supplemental Figure S7. K^+ contents and analysis of K^+ fluxes at the plasma membrane and tonoplast.

Supplemental Table S1. Primers used for quantitative PCR analysis of transcript abundance.

Supplemental Appendix S1.

Supplemental References S1.

ACKNOWLEDGMENTS

We thank Jaakko Kangasjärvi (University of Helsinki) for seeds of the *slac1-1* mutant and *pSLAC1*:*SLAC1*-complemented lines as well as Christopher Grefen and Anna Amtmann (University of Glasgow) for comments during preparation of the manuscript.

Received September 20, 2012; accepted October 20, 2012; published October 22, 2012.

LITERATURE CITED

Ache P, Becker D, Ivashikina N, Dietrich P, Roelfsema MRG, Hedrich R (2000) GORK, a delayed outward rectifier expressed in guard cells of *Arabidopsis thaliana*, is a K^+-selective, K^+-sensing ion channel. FEBS Lett **486:** 93–98

Allen GJ, Chu SP, Harrington CL, Schumacher K, Hoffmann T, Tang YY, Grill E, Schroeder JI (2001) A defined range of guard cell calcium oscillation parameters encodes stomatal movements. Nature **411:** 1053–1057

Amtmann A, Blatt MR (2009) Regulation of macronutrient transport. New Phytol **181:** 35–52

Barbier-Brygoo H, De Angeli A, Filleur S, Frachisse JM, Gambale F, Thomine S, Wege S (2011) Anion channels/transporters in plants: from molecular bases to regulatory networks. Annu Rev Plant Biol **62:** 25–51

Betts RA, Boucher O, Collins M, Cox PM, Falloon PD, Gedney N, Hemming DL, Huntingford C, Jones CD, Sexton DMH, et al (2007) Projected increase in continental runoff due to plant responses to increasing carbon dioxide. Nature **448:** 1037–1041

Blatt MR (1987a) Electrical characteristics of stomatal guard cells: the contribution of ATP-dependent, "electrogenic" transport revealed by current-voltage and difference-current-voltage analysis. J Membr Biol **98:** 257–274

Blatt MR (1987b) Electrical characteristics of stomatal guard cells: the ionic basis of the membrane potential and the consequence of potassium chloride leakage from microelectrodes. Planta **170:** 272–287

Blatt MR (1988) Potassium-dependent bipolar gating of potassium channels in guard cells. J Membr Biol **102:** 235–246

Blatt MR (1992) K^+ channels of stomatal guard cells: characteristics of the inward rectifier and its control by pH. J Gen Physiol **99:** 615–644

Blatt MR (2000) Cellular signaling and volume control in stomatal movements in plants. Annu Rev Cell Dev Biol **16:** 221–241

Blatt MR, Armstrong F (1993) K^+ channels of stomatal guard cells: abscisic acid-evoked control of the outward rectifier mediated by cytoplasmic pH. Planta **191:** 330–341

Blatt MR, Gradmann D (1997) K^+-sensitive gating of the K^+ outward rectifier in *Vicia* guard cells. J Membr Biol **158:** 241–256

Blatt MR, Slayman CL (1983) KCl leakage from microelectrodes and its impact on the membrane parameters of a nonexcitable cell. J Membr Biol **72:** 223–234

Chen ZH, Eisenach C, Xu XQ, Hills A, Blatt MR (2012a) Protocol: optimised electrophysiological analysis of intact guard cells from Arabidopsis. Plant Methods **8:** 15

Chen ZH, Hills A, Bätz U, Amtmann A, Lew VL, Blatt MR (2012b) Systems dynamic modeling of the stomatal guard cell predicts emergent behaviors in transport, signaling, and volume control. Plant Physiol **159:** 1235–1251

Chen ZH, Hills A, Lim CK, Blatt MR (2010) Dynamic regulation of guard cell anion channels by cytosolic free Ca^{2+} concentration and protein phosphorylation. Plant J **61:** 816–825

De Angeli A, Monachello D, Ephritikhine G, Frachisse JM, Thomine S, Gambale F, Barbier-Brygoo H (2006) The nitrate/proton antiporter AtCLCa mediates nitrate accumulation in plant vacuoles. Nature **442:** 939–942

Dettmer J, Hong-Hermesdorf A, Stierhof YD, Schumacher K (2006) Vacuolar H^+-ATPase activity is required for endocytic and secretory trafficking in *Arabidopsis*. Plant Cell **18:** 715–730

Dodd AN, Gardner MJ, Hotta CT, Hubbard KE, Dalchau N, Love J, Assie JM, Robertson FC, Jakobsen MK, Gonçalves J, et al (2007) The *Arabidopsis* circadian clock incorporates a cADPR-based feedback loop. Science **318:** 1789–1792

Eamus D, Shanahan ST (2002) A rate equation model of stomatal responses to vapour pressure deficit and drought. BMC Ecol **2:** 8

Eisenach C, Chen ZH, Grefen C, Blatt MR (2012) The trafficking protein SYP121 of Arabidopsis connects programmed stomatal closure and K^+ channel activity with vegetative growth. Plant J **69:** 241–251

Fairley-Grenot K, Assmann SM (1991) Evidence for G-protein regulation of inward potassium ion channel current in guard cells of fava bean. Plant Cell **3:** 1037–1044

Farquhar GD, Wong SC (1984) An empirical model of stomatal conductance. Aust J Plant Physiol **11:** 191–209

Felle HH, Hepler PK (1997) The cytosolic Ca^{2+} concentration gradient of *Sinapis alba* root hairs as revealed by Ca^{2+}-selective microelectrode tests and fura-dextran ratio imaging. Plant Physiol **114:** 39–45

Garcia-Mata C, Gay R, Sokolovski S, Hills A, Lamattina L, Blatt MR (2003) Nitric oxide regulates K^+ and Cl^- channels in guard cells through a subset of abscisic acid-evoked signaling pathways. Proc Natl Acad Sci USA **100:** 11116–11121

Gedney N, Cox PM, Betts RA, Boucher O, Huntingford C, Stott PA (2006) Detection of a direct carbon dioxide effect in continental river runoff records. Nature **439:** 835–838

Gobert A, Isayenkov S, Voelker C, Czempinski K, Maathuis FJM (2007) The two-pore channel TPK1 gene encodes the vacuolar K^+ conductance and plays a role in K^+ homeostasis. Proc Natl Acad Sci USA **104:** 10726–10731

Grabov A, Blatt MR (1997) Parallel control of the inward-rectifier K^+ channel by cytosolic-free Ca^{2+} and pH in *Vicia* guard cells. Planta **201:** 84–95

Grabov A, Blatt MR (1998) Membrane voltage initiates Ca^{2+} waves and potentiates Ca^{2+} increases with abscisic acid in stomatal guard cells. Proc Natl Acad Sci USA **95:** 4778–4783

Grabov A, Blatt MR (1999) A steep dependence of inward-rectifying potassium channels on cytosolic free calcium concentration increase evoked by hyperpolarization in guard cells. Plant Physiol **119:** 277–288

Gutierrez L, Mauriat M, Guénin S, Pelloux J, Lefebvre JF, Louvet R, Rusterucci C, Moritz T, Guerineau F, Bellini C, et al (2008) The lack of a systematic validation of reference genes: a serious pitfall undervalued in reverse transcription-polymerase chain reaction (RT-PCR) analysis in plants. Plant Biotechnol J **6:** 609–618

Hamilton DWA, Hills A, Kohler B, Blatt MR (2000) Ca^{2+} channels at the plasma membrane of stomatal guard cells are activated by hyperpolarization and abscisic acid. Proc Natl Acad Sci USA **97:** 4967–4972

Haruta M, Sussman MR (2012) The effect of a genetically reduced plasma membrane protonmotive force on vegetative growth of Arabidopsis. Plant Physiol **158:** 1158–1171

Hills A, Chen ZH, Amtmann A, Blatt MR, Lew VL (2012) OnGuard, a computational platform for quantitative kinetic modeling of guard cell physiology. Plant Physiol **159:** 1026–1042

Honsbein A, Sokolovski S, Grefen C, Campanoni P, Pratelli R, Paneque M, Chen ZH, Johansson I, Blatt MR (2009) A tripartite SNARE-K^+ channel complex mediates in channel-dependent K^+ nutrition in *Arabidopsis*. Plant Cell **21:** 2859–2877

Hosy E, Vavasseur A, Mouline K, Dreyer I, Gaymard F, Porée F, Boucherez J, Lebaudy A, Bouchez D, Very A-A, et al (2003) The *Arabidopsis* outward K^+ channel GORK is involved in regulation of stomatal movements and plant transpiration. Proc Natl Acad Sci USA **100:** 5549–5554

Hoth S, Hedrich R (1999) Distinct molecular bases for pH sensitivity of the guard cell K^+ channels KST1 and KAT1. J Biol Chem **274:** 11599–11603

Jossier M, Kroniewicz L, Dalmas F, Le Thiec D, Ephritikhine G, Thomine S, Barbier-Brygoo H, Vavasseur A, Filleur S, Leonhardt N (2010) The Arabidopsis vacuolar anion transporter, AtCLCc, is involved in the regulation of stomatal movements and contributes to salt tolerance. Plant J **64:** 563–576

Lebaudy A, Vavasseur A, Hosy E, Dreyer I, Leonhardt N, Thibaud JB, Véry AA, Simonneau T, Sentenac H (2008) Plant adaptation to fluctuating environment and biomass production are strongly dependent on guard cell potassium channels. Proc Natl Acad Sci USA **105:** 5271–5276

Lopez-Marques RL, Schiott M, Jakobsen MK, Palmgren MG (2004) Structure, function and regulation of primary H^+ and Ca^{2+} pumps. *In* MR Blatt, ed, Membrane Transport in Plants, Vol 15. Blackwell, Oxford, pp 72–104

McAinsh MR, Pittman JK (2009) Shaping the calcium signature. New Phytol **181:** 275–294

McLaughlin SGA, Dilger JP (1980) Transport of protons across membranes by weak acids. Physiol Rev **60:** 825–863

Meharg AA, Blatt MR (1995) NO_3^- transport across the plasma membrane of *Arabidopsis thaliana* root hairs: kinetic control by pH and membrane voltage. J Membr Biol **145:** 49–66

Nakamura RL, McKendree WL Jr, Hirsch RE, Sedbrook JC, Gaber RF, Sussman MR (1995) Expression of an Arabidopsis potassium channel gene in guard cells. Plant Physiol **109:** 371–374

Negi J, Matsuda O, Nagasawa T, Oba Y, Takahashi H, Kawai-Yamada M, Uchimiya H, Hashimoto M, Iba K (2008) CO_2 regulator *SLAC1* and its homologues are essential for anion homeostasis in plant cells. Nature **452:** 483–486

Peiter E, Maathuis FJM, Mills LN, Knight H, Pelloux J, Hetherington AM, Sanders D (2005) The vacuolar Ca^{2+}-activated channel TPC1 regulates germination and stomatal movement. Nature **434:** 404–408

Pilot G, Lacombe B, Gaymard F, Cherel I, Boucherez J, Thibaud JB, Sentenac H (2001) Guard cell inward K^+ channel activity in *Arabidopsis* involves expression of the twin channel subunits KAT1 and KAT2. J Biol Chem **276:** 3215–3221

Rasband WS, Bright DS (1995) NIH IMAGE: a public domain image-processing program for the Macintosh. Microbeam Anal **4:** 137–149

Sanders D, Hopgood M, Jennings IR (1989) Kinetic response of H^+-coupled transport to extracellular pH: critical role of cytosolic pH as a regulator. J Membr Biol **108:** 253–261

Schachtman DP, Schroeder JI, Lucas WJ, Anderson JA, Gaber RF (1992) Expression of an inward-rectifying potassium channel by the *Arabidopsis* KAT1 cDNA. Science **258:** 1654–1658

Schroeder JI, Allen GJ, Hugouvieux V, Kwak JM, Waner D (2001) Guard cell signal transduction. Annu Rev Plant Physiol Plant Mol Biol **52:** 627–658

Siegel RS, Xue SW, Murata Y, Yang YZ, Nishimura N, Wang A, Schroeder JI (2009) Calcium elevation-dependent and attenuated resting calcium-dependent abscisic acid induction of stomatal closure and abscisic acid-induced enhancement of calcium sensitivities of S-type anion and inward-rectifying K channels in Arabidopsis guard cells. Plant J **59:** 207–220

Speksnijder JE, Miller AL, Weisenseel MH, Chen T-H, Jaffe LF (1989) Calcium buffer injections block fucoid egg development by facilitating calcium diffusion. Proc Natl Acad Sci USA **86:** 6607–6611

Vahisalu T, Kollist H, Wang YF, Nishimura N, Chan WY, Valerio G, Lamminmäki A, Brosché M, Moldau H, Desikan R, et al (2008) SLAC1 is required for plant guard cell S-type anion channel function in stomatal signalling. Nature **452:** 487–491

Wang Y, Blatt MR (2011) Anion channel sensitivity to cytosolic organic acids implicates a central role for oxaloacetate in integrating ion flux with metabolism in stomatal guard cells. Biochem J **439:** 161–170